Pramana – J. Phys. (2017) 88: 24
DOI 10.1007/s12043-016-1327-2

Hybrid combination of multi-layer perceptron and neutron activation analysis in cement prediction

E EFTEKHARI-ZADEH[1,*], S A H FEGHHI[2] and G H ROSHANI[3]

[1]Young Researchers and Elite Club, Kermanshah Branch, Islamic Azad University, Kermanshah, Iran
[2]Radiation Application Department, Shahid Beheshti University, Tehran, Iran
[3]Department of Electrical Engineering, Kermanshah University of Technology, Kermanshah, Iran
*Corresponding author. E-mail: e.eftekharizade@yahoo.com

MS received 19 January 2016; revised 17 May 2016; accepted 17 June 2016; published online 4 January 2017

Abstract. Determination of concentration of major elements such as Ca, Si, Al, and Fe in cement is very important for quality control during its production, correct classification according to the existing standards, and thus for appropriate use in the construction industry. For this purpose, neutron activation analysis is very suitable. In this preliminary theoretical work, the irradiation and consecutive measurement of the percentage of the constituent elements in different cement samples were done using MCNPX with γ-ray spectra as the output. Specific peaks of Ca, Si, Al, and Fe obtained from these spectra were used as input for artificial neural network (18 of them for training and 8 for testing) resulting in the determination of each element in the given sample. The mean absolute errors of the results are less than 0.4%, which is very promising for the future experimental work where the uncertainties are usually one order higher.

Keywords. Cement; artificial neural network; MCNPX; neutron activation analysis.

PACS Nos 24.10.Lx; 24; 24.10.−i

1. Introduction

Neutron activation analysis (NAA) is an important method for the qualitative and quantitative analyses of many major, minor, trace, and rare elements in materials of different matrices. The method is highly specific as it is based on the characteristics of induced radionuclides, representing completely independent nuclear principle, in contrast to the electron nature of most of the other analytical (chemical) methods. More than 60 elements can be determined using different techniques with detection limits down to 10^{-6} mg/kg for some elements [1–4].

NAA is a suitable method for the analysis of different types of cement using reactor, inertial electrostatic confinement fusion (IECF) or other isotopic neutron sources [5–11]. Accurate elemental characterizations of cement samples are of great interest due to the importance of cement in the construction industry. Percentage of major elements in cement is very important for quality control during its production, correct classification according to the existing standards, and thus for appropriate use in construction industry. For example, percentage of MgO is limited to 6% maximum by weight for Portland cements, because it can impact soundness at higher levels [12]. Gypsum ($CaSO_4$) is added to cement to regulate the setting time, but too much gypsum can cause expansion and, therefore, SO_3 is generally limited to 3.5%. The alkali content of cement (mostly chloride) is reflected in the amounts of potassium oxide (K_2O) and sodium oxide (Na_2O). Large amounts can cause certain difficulties in regulating setting time. Low alkali cements, when used with calcium chloride in concrete, can cause discolouration in trowelled flatwork surfaces. ASTM has an optional limit in total alkalies of 0.6%, calculated by the equation $Na_2O + 0.658K_2O$ [13]. Chlorides in concrete result in the corrosion of reinforcing steel. Steel is naturally protected (passivated) from corrosion in the high pH (alkaline) environment when embedded in concrete. When chloride ions are present near the reinforcing steel, they override this passivation causing corrosion. This is the most common cause of corrosion. However, even for plain concrete, it is prudent to limit the chloride content to 1% by weight of cement [14].

Artificial neural network (ANN) has been used many times in nuclear techniques due to its classification, clustering, and prediction abilities. ANN can be used in artificial intelligence techniques for detecting drugs and explosives using neutron computerized tomography [15], for unfolding the neutron spectrum of a NE213 scintillator [16] for determining neutron fluence-to-dose conversion coefficients [17], flow and heat transfer problems in nuclear engineering [18] etc. These techniques have been widely used in gamma densitometry and flow measurement [19–23]. In the field of activation analysis, Nunes *et al* [24] used ANN for detecting explosive materials using prompt gamma neutron activation analysis (PGNAA) and Doostmohammadi *et al* [25] used this method to simulate qualitative PGNAA. The use of ANN in classical mode of NAA is therefore very promising as the γ-ray spectra to be evaluated are much less complicated than in the case of PGNAA. In this study, different percentages of cement irradiated by fission neutron source were simulated using MCNPX and specific γ-rays were obtained. Four specific peaks of these spectra were considered as the inputs of ANN and the percentage of each element was considered as the output.

2. Methods

2.1 *Monte Carlo simulation*

MCNPX version 2.7 is a Monte Carlo [26] radiation-transport code which uses three-dimensional (3D) geometry modelling, continuous-energy transport, transport of 34 different particle types, a variety of source and tally options, and interactive graphics. In this work, a newly added feature, 'ACT card' of this code was used to simulate the generated spectra in NAA analysis [27].

Twenty six cement samples with dimensions of $10\times10\times4$ cm were added into MCNPX input file, each with different concentrations of constituent elements (different types of Portland cement). The irradiation was simulated by a 100 mCi neutron source with Watt fission spectrum (in order to define ^{252}Cf spontaneous fission neutron source). In order to focus all the emitted neutrons in one direction to the sample, so that the neutron flux is increased, the beryllium collimator was placed around the neutron source. The exact experimental set-up is depicted in figure 1. To avoid spectral interferences, only interactions with fast neutrons were considered, e.g. ^{27}Al$(n,\ p)^{27}$Mg. Only photons and neutrons were considered and importance factor 1 was assigned for all the cells. Gamma-ray spectra were created using F1 tally on the sphere centred at the target with 50 cm radius. For this purpose, a model of HPGe detector [28] with 8192 energy (up to 4 MeV) channels was used. The cooling and counting times of 30 s and 1 h were set, respectively. Typical γ-ray spectrum for a cement sample simulated by MCNPX is shown in figure 2.

2.2 *Artificial neural network*

Artificial neural network (ANN) is based on the operation of biological neural networks. The fundamental

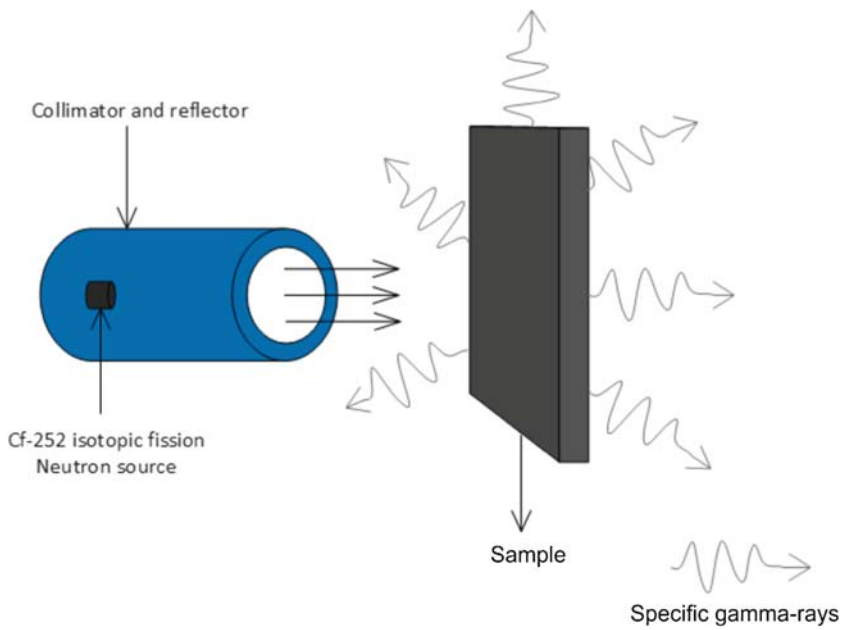

Figure 1. The irradiation set-up.

processing element of ANN is an artificial neuron [29]. Neural networks are tools for non-linear data modelling. They can be used to model complex relationships between the inputs and the outputs or to find patterns in the given data [30]. The major advantage of the neural network approach is that most of the intense computation takes place during the training process before the analysis [31], and so when ANN is trained in advance, analysis operation will be faster. Multilayer perceptron (MLP) networks are the most widely used ANNs [32]. The proposed MLP model is shown in figure 3, where the inputs are peak areas of gamma photons related to Ca, Si, Fe, and Al and the outputs are the concentrations of Ca, Si, and Fe. Note that, only Ca, Si, and Fe concentrations were used as the ANN outputs and the Al content was obtained as complementary.

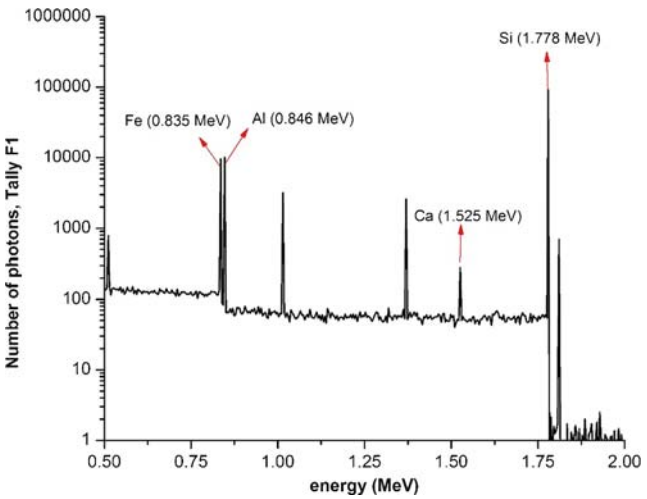

Figure 2. Typical γ-ray spectrum for a cement sample simulated by MCNPX.

Training of the given MLP network was done by Levenberg–Marquardt (LM) algorithm. In this method, first derivative and second derivative (hessian) are used for network weight correction [33].

The input to the node m in the first hidden layer is given by [29,32]

$$\eta_m = \sum_{u=1}^{4} (X_u W_{um}) + b_m, \quad m = 1, 2, 3. \tag{1}$$

The output from the mth neuron of the hidden layer is given by

$$U_m = f\left(\sum_{u=1}^{4} (X_u W_{um}) + b_m\right), \quad m = 1, 2, 3. \tag{2}$$

The output from the mth neuron in the output layer is given by

$$O = \sum_{u=1}^{3} (U_u W_{um}) + b_m, \tag{3}$$

where X is the input, b is the bias term, W is the weighting factor and f is the activation function of the hidden layers.

3. Experimental

Gamma-ray spectra were evaluated and the peak areas belonging to the specific γ-ray energies of the nuclides

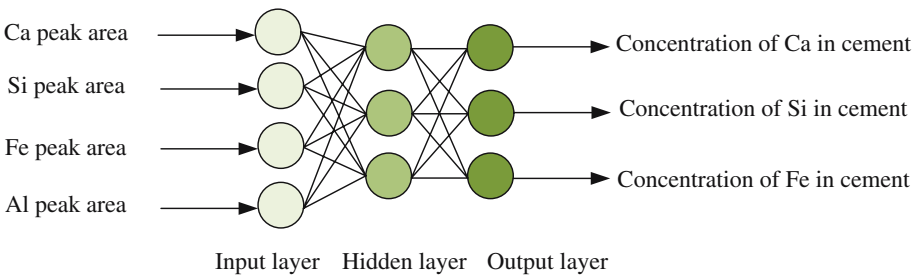

Figure 3. Architecture of the proposed MLP model.

Table 1. Selected nuclear properties of the nuclides of interest.

Radionuclide	Production mode	Half-life	Energy of interest (keV)	Intensity (%)
^{27}Mg	^{27}Al$(n, p)^{27}$Mg	9.46 min	843	71.4
^{28}Al	^{28}Si$(n, p)^{28}$Al	2.24 min	1778	100
^{42}K	^{42}Ca$(n, p)^{42}$K	12.36 h	1525	18.08
^{56}Mn	^{56}Fe$(n, p)^{56}$Mn	2.58 h	1810	27.19

of interest were used as the inputs for ANN. Only the most intensive gamma energies were used for the determination of elemental concentrations. The list of nuclides used and their nuclear features are given in table 1 [34]. The input library contained 26 members, 18 of them were used for training and the rest for testing. In this stage, different ANN structures were tested and optimized to obtain the best ANN configuration. Many different structures with one, two and three hidden layers with different number of neurons in each layer were tested. MATLAB 8.1.0.604 software was used for training the ANN model. Table 2 shows the specification of the proposed ANN model used in this study.

Table 2. Specification of the proposed ANN model.

Neural network	MLP
Number of neurons in the input layer	4
Number of neurons in the first hidden layer	3
Number of neurons in the output layer	3
Number of epochs	100
Activation function	Tangent sigmoid

4. Results and discussion

The comparison between the simulated (MCNPX) and the predicted (ANN) results for training and testing data are shown in tables 3 and 4 respectively. The

Table 3. Data used for training the network and the predicted outputs.

Peak area related to Ca	Peak area related to Si	Peak area related to Fe	Peak area related to Al	Content of Ca	Content of Si	Content of Fe	Predicted output of Ca	Predicted output of Si	Predicted output of Fe
282	92377	9631	10122	65	22	8	64.99	22.00	7.96
278	83752	9632	10065	67	20	8	66.97	20.01	8.03
259	66867	9405	9937	71	16	8	71.04	16.02	7.94
253	58387	9479	9887	73	14	8	72.93	14.00	8.02
283	92542	2508	17343	65	22	2	65.02	21.98	2.00
281	92462	7289	12587	65	22	6	64.94	21.99	6.02
282	92377	9631	10122	65	22	8	64.99	22.00	7.96
274	92342	12203	7624	65	22	10	64.95	21.99	10.07
270	92287	14540	5099	65	22	12	65.06	22.00	11.96
252	55973	12005	13651	70	13	10	70.02	12.99	9.99
265	63281	11990	10573	70	15	10	70.02	14.97	10.01
264	70808	11935	7511	70	17	10	70.03	16.97	9.99
267	77297	12262	13856	65	18	10	64.90	18.01	9.99
260	76311	9527	13140	67	18	8	67.05	17.99	7.99
260	74410	4762	11756	71	18	4	71.02	17.98	4.02
265	73515	2416	11087	73	18	2	72.94	18.00	1.99
283	92542	2508	17343	65	22	2	65.02	21.98	2.00
277	83994	4778	14894	67	20	4	67.02	20.03	3.98

Table 4. Data used for testing the network and the predicted outputs.

Peak area related to Ca	Peak area related to Si	Peak area related to Fe	Peak area related to Al	Content of Ca	Content of Si	Content of Fe	Predicted output of Ca	Predicted output of Si	Predicted output of Fe
264	75197	9461	10006	69	18	8	69.08	17.98	7.96
273	92515	4854	14979	65	22	4	65.02	21.96	4.00
254	48243	12095	16713	70	11	10	70.04	10.97	9.95
259	50037	9504	9825	75	12	8	74.78	12.07	8.00
271	75432	7175	12434	69	18	6	68.97	18.03	6.05
271	75432	7175	12434	69	18	6	68.97	18.03	6.05
270	78246	12064	4441.4	70	19	10	69.95	18.96	10.07
266	72590	87	10432	75	18	0	74.83	17.99	0.03

Table 5. Comparison between the simulated and the predicted results used for validation.

Peak area related to Ca	Peak area related to Si	Peak area related to Fe	Peak area related to Al	Content of Ca	Content of Si	Content of Fe	Predicted output of Ca	Predicted output of Si	Predicted output of Fe
271	82174	5952	9085	70	20	5	70.03	19.96	4.95
261	62905	5960	13509	72	15	5	71.93	15.06	5.09
259	66867	9405	9937	71	16	8	71.04	16.02	7.94
253	58161	11846	7432	73	14	10	72.97	13.97	9.94
253	49474	14228	4929	75	12	12	74.87	11.96	11.79

Ca, Si, and Fe contents predicted by ANN model are close to the simulated results. In order to show the accuracy of the results, a validation set was defined in addition to the training and testing set. Results for this set are given in table 5 which indicate that the network is highly precise.

Such results show that, in the future, ANN can be used as an accurate and reliable model for predicting elemental contents based on the information obtained from neutron activation procedure.

The errors obtained for the proposed ANN model are shown in table 6, where the mean relative error percentage (MRE%), the root mean square error (RMSE), and the mean absolute error percentage (MAE) of the network are calculated by

$$\mathrm{MRE\%} = 100 \times \frac{1}{N}\sum_{j=1}^{N}\left|\frac{X_j(\mathrm{Sim}) - X_j(\mathrm{Pred})}{X_j(\mathrm{Sim})}\right|, \quad (4)$$

$$\mathrm{RMSE} = \left[\frac{\sum_{j=1}^{N}(X_j(\mathrm{Sim}) - X_j(\mathrm{Pred}))^2}{N}\right]^{0.5}, \quad (5)$$

$$\mathrm{MAE} = \frac{1}{N}\sum_{j=1}^{N}\left|X_j(\mathrm{Sim}) - X_j(\mathrm{Pred})\right|, \quad (6)$$

where N is the number of members and $X(\mathrm{Sim})$ and $X(\mathrm{Pred})$ stand for simulated (MCNPX) and predicted (ANN) values respectively.

The efficiency and ability of a typical network is examined by defined errors and regression diagrams. The more precise the given network is, the closer the data to the $x = y$ line lies. Very low errors of the training set in the presented network show the precision of the prediction and low errors of the testing set show the accuracy of the method.

The aim of this study is to propose the MLP as an efficient tool for predicting constituent elements in cement. This method can be useful in real conditions, too. In experimental conditions, the uncertainty of data is one of the most important issues. In this study, the uncertainty of data was less than 5% and the inputs of ANN do not overlap. Another important advantage is that the background radiation can be eliminated.

Table 6. Errors for training and testing results of the proposed ANN model.

	Error	Train	Test
Ca Output	MRE%	0.0001	0.0636
	MAE	0.0556	0.1136
	RMSE	0.0006	0.0015
Si Output	MRE%	0.0002	0.0176
	MAE	0.0614	0.1583
	RMSE	0.0007	0.0019
Fe Output	MRE%	0.0018	0.1624
	MAE	0.2228	0.3773
	RMSE	0.0030	0.0043

5. Conclusion

Artificial neural network is very promising in handling problems of modelling, prediction, control, and classification. Its use can solve the problems of manual evaluation of experimental data and automate and speed up the whole process of elemental analysis in the near future. It was proved by this preliminary theoretical study that for simple sample matrices (cement) and ideal irradiation/counting conditions, the ANN could work. As the next step, the experimental work with analyses of suitable simple matrix samples in ideal conditions should be held to obtain experience with real spectra and to further develop the model.

Acknowledgements

The authors would like to thank Ing. Marie Kubešová, Ph.D. from Nuclear Physics Institute of the Czech Academy of Sciences for her valuable comments.

References

[1] M Blaauw, *The holistic analysis of gamma-ray spectra in instrumental neutron activation analysis* (The Interfaculty Reactor Institute Delft, Netherlands, 1993)

[2] P Bode, *Instrumental and organizational aspects of a neutron activation analysis laboratory* (The Interfaculty Reactor Institute Delft, Netherlands, 1996)

[3] Use of research reactors for neutron activation analysis, IAEA-TECDOC-1215, IAEA Vienna, 2001

[4] F De Corte, *The k_0-standardization method, A move to the optimization of neutron activation analysis* (University of Gent, Belgium, 1987)

[5] R J Muhyedeen Bahjat, F I Kanbour and S M Al-Jubori, *Iraqi J. Sci. A* **42**, 1 (2001)

[6] M Ali-Abdallah, N A Mansour, M A Ali and M Fayez-Hassan, *Adv. Appl. Sci. Res.* **2(4)**, 613 (2011)

[7] F A Iddings *et al*, *Nuclear techniques for cement determination*, U.S. Clearinghouse fed. Sci. fech. Infrompb rep. Pb-178464:73 (1968)

[8] J Kuusi, *Nucl. Appl. Technol.* **8**, 465 (1970)

[9] Y S Khrbish, I O Abugassa, N Benfaid and A A Bashir, *J. Radioanal. Nucl. Chem.* **271**, 63 (2007)

[10] E Eftekhari Zadeh, S A H Feghhi and E Bayat, *Radiochem.* **58(2)**, 216 (2016)

[11] E Eftekhari Zadeh, A Sadighzadeh, A Salehizadeh, E Nazemi and G H Roshani, *Anal. Meth.* **8**, 2510 (2016)

[12] American Society for Testing and Materials (ASTM) C150 / C150M – 2012. Standard Specification for Portland Cement, ⟨http://www.astm.org/Standards/C150.htm⟩

[13] http://www.continentalcement.com/web/technical/uploads/Cement_Properties_and_Characteristics.pdf downloaded 1.5.2016

[14] http://www.nrmca.org/aboutconcrete/downloads/Tip13.pdf downloaded 1.5.2016

[15] F J O Ferreira, V R Crispim and A X Silva, *Appl. Radiat. Isot.* **68**, 1012 (2010)

[16] A Sharghi Ido, M R Bonyadi, G R Etaati and M Shahriari, *Appl. Radiat. Isot.* **67**, 1912 (2009)

[17] V M Hernandez-Davila, T G Soto-Bernal and H R Vega-Carrillo, *Appl. Radiat. Isot.* **83**, 249 (2014)

[18] T Cong, G Su, S Qiu and W Tian, *Prog. Nucl. Energy* **62**, 54 (2013)

[19] M Khorsandi and S A H Feghhi, *Measurement* **44**, 1512 (2011)

[20] G H Roshani, S A H Feghhi, A Adineh-Vand and M Khorsandi, *Measurement* **46**, 3276 (2013)

[21] C M Salgado, L E B Brandao, R Schirru, C M N A Pereira, A Xavier da Silva and R Ramos, *Appl. Radiat. Isot.* **67**, 1812 (2009)

[22] C M Salgado, C M N A Pereira, R Schirru and L E B Brandao, *Prog. Nucl. Energy* **52**, 555 (2010)

[23] E Nazemi, G H Roshani, S A H Feghhi, S Setayeshi, E Eftekhari Zadeh and A Fatehi, *Int J. Hydrogen Energy* **41(18)**, 7438 (2016)

[24] W V Nunes, A X da Silva, V R Crispim and R Schirru, *Appl. Radiat. Isot.* **56**, 937 (2002)

[25] V Doostmohammadi, D Sardari and A M Nasrabadi, *J. Radioanal. Nucl. Chem.* **283**, 403 (2010)

[26] D B Pelowitz *et al*, MCNPX 2.7.E Extensions, Los Alamos National Laboratory Report LA-UR-11-01502 (2011)

[27] J W Durkee Jr, M R James, G W McKinney, H R Trellue, L S Waters and W B Wilson, *Prog. Nucl. Energy* **51**, 828 (2009)

[28] E Eftekhari Zadeh, S A H Feghhi, E Bayat and G H Roshani. *J. Exp. Phys.* **2014**, Article ID 623683, 4 pages, DOI: 10.1155/2014/623683 (2014)

[29] J G Taylor, *Neural networks and their applications* (John Wiley & Sons Ltd, West Sussex, UK, 1996)

[30] K Gurney, *An introduction to neural networks* (University College London (UCL) Press, London, 1997)

[31] S Haykin, *Neural networks*: *A comprehensive foundation* (Prentice Hall, Englewood Cliffs, NJ, 1999)

[32] A R Gallant and H White, *Neural Networks* **5**, 129 (1992)

[33] M T Hagan and M Menhaj, *IEEE Trans. Neural Networks* **5**, 989 (1994)

[34] IAEA-TECDOC-564, Practical aspects of operating a neutron activation analysis laboratory (1990)